Vascular endothelial tyrosine phosphatase (VE-PTP)-null mice undergo vasculogenesis but die embryonically because of defects in angiogenesis

Melissa G. Dominguez, Virginia C. Hughes, Li Pan, Mary Simmons, Christopher Daly, Keith Anderson, Irene Noguera-Troise, Andrew J. Murphy, David M. Valenzuela, Samuel Davis, Gavin Thurston, George D. Yancopoulos*, and Nicholas W. Gale*

Regeneron Pharmaceuticals, Inc., 777 Old Saw Mill River Road, Tarrytown, NY 10591

Contributed by George D. Yancopoulos, December 28, 2006 (sent for review December 21, 2006)

Development of the vascular system depends on the highly coordinated actions of a variety of angiogenic regulators. Several of these regulators are members of the tyrosine kinase superfamily, including VEGF receptors and angiopoietin receptors, Tie1 and Tie2. Tyrosine kinase signaling is counter-regulated by the activity of tyrosine phosphatases, including vascular endothelial protein tyrosine phosphatase (VE-PTP), which has previously been shown to modulate Tie2 activity. We generated mice in which VE-PTP is replaced with a reporter gene. We confirm that VE-PTP is expressed in endothelium and also show that VE-PTP is highly expressed in the developing outflow tract of the heart and later is expressed in developing heart valves. Vasculogenesis occurs normally in mice lacking VE-PTP; however, angiogenesis is abnormal. Angiogenic defects in VE-PTP-null mice were most pronounced in the yolk sac and include a complete failure to elaborate the primitive vascular scaffold into higher-order branched arteries, veins, and capillaries. VE-PTP continues to be expressed into adulthood in the vasculature and heart valves, suggesting later roles in vascular development or homeostasis. VE-PTP is also expressed in the vasculature of growing tumors, suggesting that VE-PTP may be a new potential target for angiogenic therapies.

gene targeting | tyrosine kinase | Tie2

During embryonic development, endothelial cells (ECs) form the first blood vessels, a primary capillary plexus in extraembryonic tissue, by a process termed vasculogenesis (1). The primitive heart, paired dorsal aortas, and vitelline vessels also form during this stage by the convergence of newly differentiated ECs. As the heart begins to beat, the vascular system remodels, expands, and differentiates from a primitive undifferentiated plexus into a hierarchy of arteries, veins, and capillaries by the process known as angiogenesis. Significant disruption of vasculogenesis or angiogenesis leads to embryonic lethality, as is observed when genes involved in vascular development are perturbed. Several families of molecules, which are expressed in vascular endothelium, are critical to these processes. These include VEGF and its receptors VEGF-R1, -R2, and -R3, which have been shown to be critical in the earliest stages of vasculogenesis, as well as later in angiogenesis, and the angiopoietin/Tie, ephrin/Eph, TGF-β/TGF-β receptor and Delta/Notch families, shown to be critical for angiogenesis (summarized in ref. 2).

Several of these critical molecular players in vasculogenesis and angiogenesis are members of the receptor tyrosine kinase superfamily, which mediates signal transduction by tyrosine phosphorylation of signaling intermediates and effector molecules. Transduction of signals by tyrosine phosphorylation is counter-regulated by a variety of transmembrane and cytoplasmic protein tyrosine phosphatases (PTPs), a few of which are known to be expressed in ECs. One of these PTPs, CD148/DEP-1/PTPη, causes vascular defects and embryonic lethality when mutated, although its expression is not restricted to ECs (3). The only known PTP whose expression appears to be restricted to vascular ECs in embryos is vascular endothelial PTP (VE-PTP) (4). VE-PTP, the mouse homologue of receptor-type human PTP-β (5), has been shown to associate with and dephosphorylate Tie2 (4) and VE-cadherin (6) but was shown to not interact with VEGF-R2 (4).

To study the expression pattern in embryonic and adult tissues and to elucidate the functional role of VE-PTP in vascular development, we generated mice in which the VE-PTP gene was replaced by LacZ, a high-resolution reporter gene. LacZ expression confirms that VE-PTP is expressed in both arterial and venous vascular endothelium in embryos, although more strongly in arterial vessels. We also show that, early in development, VE-PTP is highly expressed in the outflow tract and later in the valves of the heart. VE-PTP continues to be expressed in adult vascular endothelium and is also expressed in tumor vasculature.

VE-PTP-null mice die embryonically because of a variety of angiogenesis defects in the embryo and the yolk sac. Defects include failure of remodeling of the vascular plexus into large veins and branched vascular networks, which is clear throughout the embryo but is most prominent in the yolk sac. Our findings show that VE-PTP is essential for cardiovascular development, and its continued expression in the adult suggests it may also have a role in vascular homeostasis and may be involved in the pathological angiogenesis of tumors.

Although the genetic deletion in VE-PTP described here is distinct, the vascular phenotype is essentially the same as that described for another VE-PTP mutant published during the preparation of this manuscript (7). Baumer *et al.* (7) describe a mutation in VE-PTP that resulted in a soluble extracellular form of VE-PTP being secreted, and that may have some neomorphic function (7, 8). However, the symmetry of our phenotype with that of Baumer *et al.* (7) suggests the phenotypes resulting from both mutations are a consequence of loss of VE-PTP function.

Results

VE-PTP Homozygous Mutant Mice Die Embryonically. VelociGene technology (9) was used to create a targeting vector in which exons 2 (except for the first 26 nucleotides, retaining the endogenous signal peptide) to 3 were replaced with a transmembrane-LacZ reporter gene and a loxP-flanked neomycin selection cassette (Fig. 1*A*). Correct gene targeting (frequency = 3.5%) in F1H4 (C57BL/

Author contributions: M.G.D., G.T., and N.W.G. designed research; M.G.D., V.C.H., L.P., M.S., I.N.-T., and N.W.G. performed research; K.A., I.N.-T., D.M.V., and N.W.G. contributed new reagents/analytic tools; M.G.D., V.C.H., L.P., C.D., K.A., A.J.M., S.D., G.T., G.D.Y., and N.W.G. analyzed data; and M.G.D. and N.W.G. wrote the paper.

Conflict of interest statement: All authors are employees of Regeneron Pharmaceuticals, Inc..

Freely available online through the PNAS open access option.

Abbreviations: EC, endothelial cell; PTP, protein tyrosine phosphatase; VE-PTP, vascular endothelial PTP; E*n*, embryonic day *n*; PECAM-1, platelet/endothelial cell adhesion molecule 1.

*To whom correspondence may be addressed. E-mail: george.yancopoulos@regeneron.com or nicholas.gale@regeneron.com.

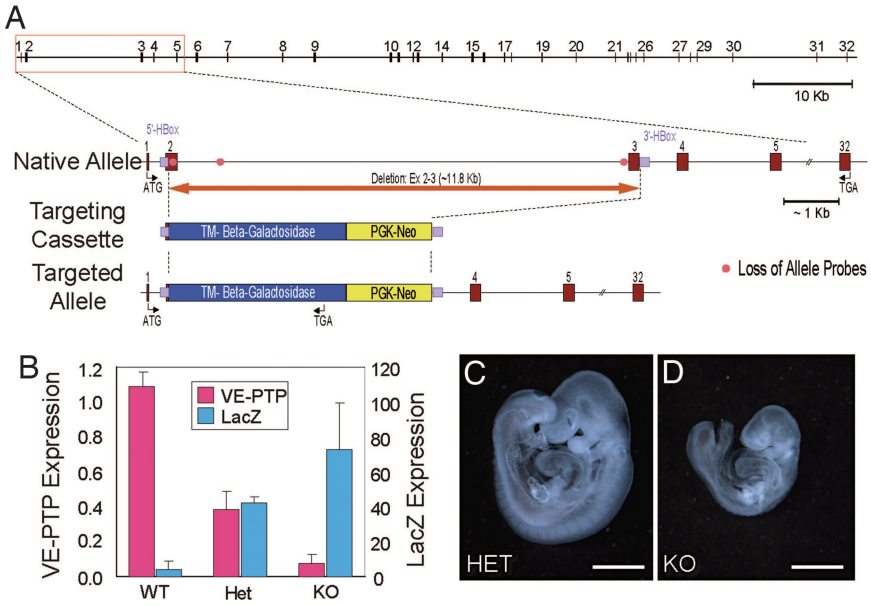

Fig. 1. Gene targeting and embryo phenotype. (*A*) A schematic representation of the VE-PTP targeting strategy. An 11.8-kb VE-PTP genomic region along with flanking homology sequence (HBox) was used for bacterial homologous recombination with VelociGene technology (9). A TM-β-gal/PGK-Neo reporter cassette was inserted, deleting from 27 nucleotides (in exon 2) through exon 3 in the targeted allele. (*B*) Quantitative RT-PCR results of transcript levels of VE-PTP and lacZ with E9.5 embryo RNA from WT ($n = 3$), VE-PTP$^{Lz/+}$ (Het, $n = 3$), and VE-PTP$^{Lz/Lz}$ (knockout, $n = 4$). The relative VE-PTP and LacZ expression levels are graphed on separate scales. (*C* and *D*) Freshly dissected E9.5 embryos, showing the growth retardation, large heart, and pericardial edema phenotypes seen in the VE-PTP$^{Lz/Lz}$ embryo (*D*) compared with VE-PTP$^{Lz/+}$ (*C*).

6:129 hybrid) ES cell clones was scored by using the loss of native allele assay (data not shown, and see ref. 9). Male chimeric mice (complete transmitters of ES cell-derived sperm) from two independent ES cell clones were bred to C57BL/6 mice to generate F_1 offspring heterozygous for the modified VE-PTP allele (VE-PTP$^{Lz/+}$). When F_1 animals were intercrossed to generate F_2 offspring, no pups homozygous for the modified VE-PTP allele (VE-PTP$^{Lz/Lz}$) were born out of 25 litters (174 mice; 62% VE-PTP$^{Lz/+}$, 37% WT), leading to the suspicion that homozygous deletion of VE-PTP results in embryonic death. Timed matings of VE-PTP$^{Lz/+}$ mice were used to generate embryos 8.5–10.5 days postcoitum [embryonic day (E) 8.5–10.5]. Up to E9.5, VE-PTP$^{Lz/Lz}$, VE-PTP$^{Lz/+}$, and WT littermate embryos were obtained at approximate Mendelian ratios. However, by E9.5, the VE-PTP$^{Lz/Lz}$ embryos exhibited obvious abnormalities (see below). The VE-PTP$^{Lz/+}$ and WT embryos are phenotypically indistinguishable and were both used as normal controls throughout this study.

To confirm that the loss of VE-PTP alleles results in the loss of VE-PTP mRNA expression and acquisition of LacZ expression, quantitative RT-PCR analysis was performed on E9.5 embryos (Fig. 1*B*). As expected, WT embryos express VE-PTP, but not LacZ, whereas VE-PTP$^{Lz/+}$ embryos express LacZ and have a reduction in VE-PTP mRNA levels. VE-PTP$^{Lz/Lz}$ embryos express the LacZ reporter gene but lack VE-PTP transcripts.

At E8.5, the VE-PTP$^{Lz/Lz}$ embryos are not visibly distinguishable from their WT littermates, either by size or appearance (data not shown). However, by E9.5, the VE-PTP$^{Lz/Lz}$ embryos start dying, and no surviving embryos were recovered beyond E11. Compared with control littermates, VE-PTP$^{Lz/Lz}$ embryos appear developmentally delayed starting at E9.0 and do not appear to progress beyond the E9.0 to early E9.5 stage, based on several objective criteria, including somite number and hallmarks of forelimb development. As such, they are significantly smaller than control littermates (compare Fig. 1 *D* with *C*). VE-PTP$^{Lz/Lz}$ embryos have pericardial edema (Fig. 1*D*), which varies in severity. VE-PTP$^{Lz/Lz}$ embryos collected at E10.0 and E10.5 are mostly dead, as assessed by the lack of heartbeat, or the appearance of necrotic tissue, and can have pronounced pericardial edema (data not shown).

Angiogenic Defects in Embryos. The time of embryonic death, developmental delay, and appearance of pericardial edema observed in the VE-PTP$^{Lz/Lz}$ embryos are hallmarks of defective cardiovascular development. To evaluate the vascular system of VE-PTP mutant animals, CD-31 [platelet/EC adhesion molecule 1 (PECAM-1)] immunohistochemistry was used to visualize the vasculature in whole mounts and sections of VE-PTP$^{Lz/Lz}$ and control littermate embryos and yolk sacs. Because we observed an overall developmental retardation in VE-PTP$^{Lz/Lz}$ embryos, their vascular system was compared with stage-matched control embryos. At E8.5, when the vasculature consists primarily of a simple plexus, there is no obvious difference between VE-PTP$^{Lz/Lz}$ embryos and their normal littermates (data not shown). However, by E9.5, when the vasculature of control littermates includes clearly defined large veins and networks of branching vessels (Fig. 2*A*), VE-PTP$^{Lz/Lz}$ embryos have obvious vascular defects in areas where remodeling should take place (Fig. 2*B*). In control embryos, the vascular system has undergone extensive remodeling, as seen in the dorsal midbrain, where cephalic veins (Fig. 2*C*, blue arrowheads) and major branches of the mesencephalic artery (Fig. 2*C*, red arrowheads) can be readily distinguished. In contrast, the cephalic plexus in VE-PTP$^{Lz/Lz}$ embryos fails to remodel into a hierarchical branched vascular network and instead remains as a plexus with only minor pruning (compare Fig. 2 *D* with *C*). In the lateral aspect of the developing control embryo, the cardinal veins are well defined from the head to the heart (Fig. 2*E*). In VE-PTP$^{Lz/Lz}$ embryos (Fig. 2*F*), there is PECAM-1 staining in the correct location; however, the edges are lacy and not clearly delineated, especially in the more caudal region. Occasionally, the cardinal veins are absent in VE-PTP$^{Lz/Lz}$ embryos (data not shown). Cross sections of PECAM-1-immunostained E9.0 embryos show that the dorsal aortas in VE-PTP$^{Lz/Lz}$ embryos are much smaller and have a narrower lumen than in control littermates (compare Fig. 2 *H* with *G*), and the cardinal veins are revealed in cross section to be poorly

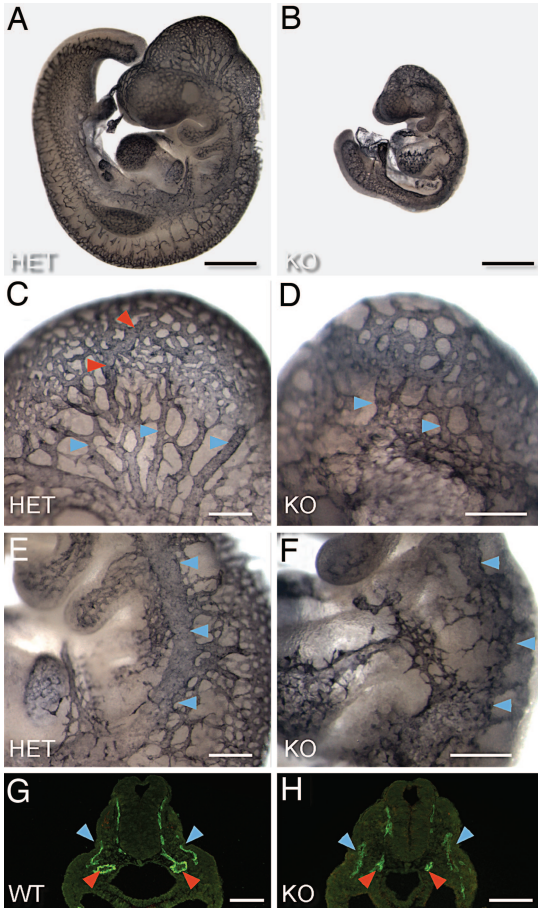

Fig. 2. Defects in vascular remodeling in VE-PTP$^{Lz/Lz}$ embryos. (*A–F*) Whole-mount PECAM-1-stained E9.5 embryos. VE-PTP$^{Lz/+}$ (*A*, *C*, and *E*) compared with a VE-PTP$^{Lz/Lz}$ littermate (*B*, *D*, and *F*). (*C* and *D*) A closeup of the head vasculature shows the normal remodeling pattern of veins (blue arrows) and arteries (red arrows) in VE-PTP$^{Lz/+}$ embryos (*C*). In VE-PTP$^{Lz/Lz}$ embryos, the venous plexus (blue arrows) undergoes only minor remodeling (*D*). (*E* and *F*) Closeup of the cardinal vein (blue arrows), which does not form correctly in VE-PTP$^{Lz/Lz}$ embryos (*F*). (*G* and *H*) PECAM-1 immunostaining of E9.0 embryo cross sections at heart level. The dorsal aortas (red arrows) are small and collapsed in VE-PTP$^{Lz/Lz}$ embryos (*H*) compared with WT (*G*), and the cardinal veins (blue arrows) are diffuse and not clearly delineated.

defined and have diffuse PECAM-1 staining, indicating incomplete remodeling.

Angiogenic Defects in Yolk Sacs. Beginning at E9.0, homozygous VE-PTP mutants can be visually identified during dissection, based on the unique appearance of their yolk sacs. Compared with control embryos, there are no visible blood-filled vessels, and the yolk sac surface appears dimpled in VE-PTP$^{Lz/Lz}$ embryos (data not shown). At E9.5, there are still no visible vessels, and the VE-PTP$^{Lz/Lz}$ yolk sac phenotype is even more obvious, because the surface is now dimpled and wrinkled (compare Fig. 3 *B* and *A*) because of a dramatic separation of the endoderm and mesoderm layers resulting from the disproportionate distention of the outer endodermal layer relative to the inner mesodermal layer (compare Fig. 3 *F* with *E*) . The severity of this yolk sac phenotype is variable, ranging from the endoderm and mesoderm layers still being fairly well connected by multiple adhesion sites, to barely being held together by sparse elongated strands of endoderm. All VE-PTP$^{Lz/Lz}$ embryos staged E9.0 or older have yolk sac defects, the severity of which was highly correlated with the severity of the vascular remodeling defects observed in the embryo proper.

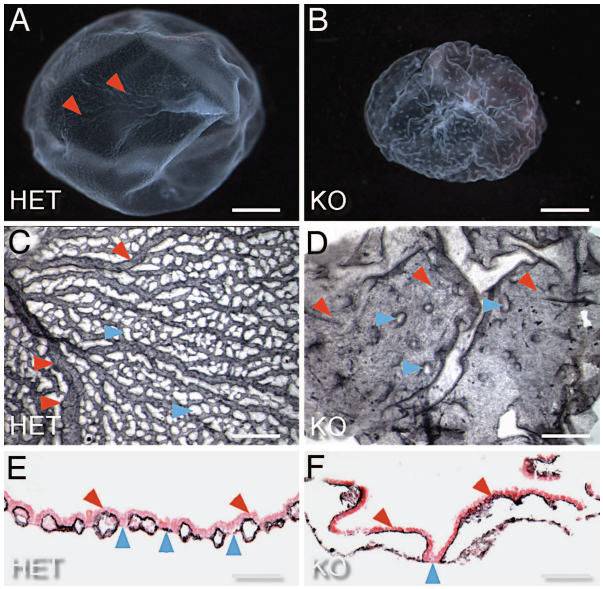

Fig. 3. Vascular defects in yolk sacs of VE-PTP$^{Lz/Lz}$ embryos. (*A* and *B*) Freshly dissected E9.5 VE-PTP$^{Lz/Lz}$ yolk sacs (*B*) can be clearly distinguished from VE-PTP$^{Lz/+}$ littermates (*A*), because of a wrinkled appearance and a lack of visible vessels, which can be seen in the yolk sacs from VE-PTP$^{Lz/+}$ littermates (*A*, red arrows). (*C* and *D*) Whole-mount PECAM-1 staining at E9.5 confirms the lack of normal vessels in VE-PTP$^{Lz/Lz}$ yolk sacs (*D*) compared with VE-PTP$^{Lz/+}$ (*C*). The endoderm and mesoderm layers in VE-PTP$^{Lz/Lz}$ yolk sacs are barely connected (*D*, blue arrows), and the entire surface is lined with PECAM-1-positive ECs (red arrows). The VE-PTP$^{Lz/+}$ yolk sacs have an organized branched network of vessels (*C*, red arrows). (*E* and *F*) PECAM-1/hematoxylin/eosin staining of E9.5 yolk sac cross sections. In VE-PTP$^{Lz/+}$ yolk sacs (*E*), the vessels are well formed (red arrows). In VE-PTP$^{Lz/Lz}$ yolk sacs (*F*), the vessels are so large (red arrows) that the endoderm and mesoderm layers are only sparsely connected (blue arrow).

To study the morphology of the developing vasculature of the yolk sac in detail, whole-mount PECAM-1 immunostaining was performed. By E9.0, the preformed primitive vascular plexus begins to be remodeled in the yolk sacs of WT and VE-PTP$^{Lz/+}$ embryos and by E9.5, the yolk sacs have an organized vascular network of branching vessels (Fig. 3*C*), which are lined with PECAM-1-positive ECs. Although the initial primitive vascular plexus forms in VE-PTP$^{Lz/Lz}$ yolk sacs, PECAM-1 immunostaining confirms the lack of any identifiable mature or remodeled blood vessels in VE-PTP$^{Lz/Lz}$ yolk sacs (Fig. 3*D*), as observed during dissection. Instead, the vessels of the primitive plexus appear to merge together. These hyperfused vessels continue to expand, to the point of almost completely separating the endoderm and mesoderm layers, except for a few remaining adhesion sites (Fig. 3 *D* and *F*). In the VE-PTP$^{Lz/Lz}$ yolk sacs with the most severe manifestation of these defects, the two layers are completely separated and held together only by sparse PECAM-1-positive strands (data not shown). However, even with this severe morphological defect, the EC layers appear intact, lining the entire surfaces of the mesoderm and endoderm layers of the yolk sac (Fig. 3 *D* and *F*), essentially making VE-PTP$^{Lz/Lz}$ yolk sacs one large endoderm- and mesoderm-enveloped blood vessel.

VE-PTP Is Expressed in Embryonic Arterial and Venous Endothelium. To determine the sites of VE-PTP expression with high resolution, VE-PTP promoter activity was followed in embryos, yolk sacs, and adult tissues of VE-PTP$^{Lz/+}$ mice by using the β-gal reporter. Consistent with the observed cardiovascular defects, VE-PTP promoter activity is restricted to the developing cardiovascular system and in particular to the vascular endothelium. A careful

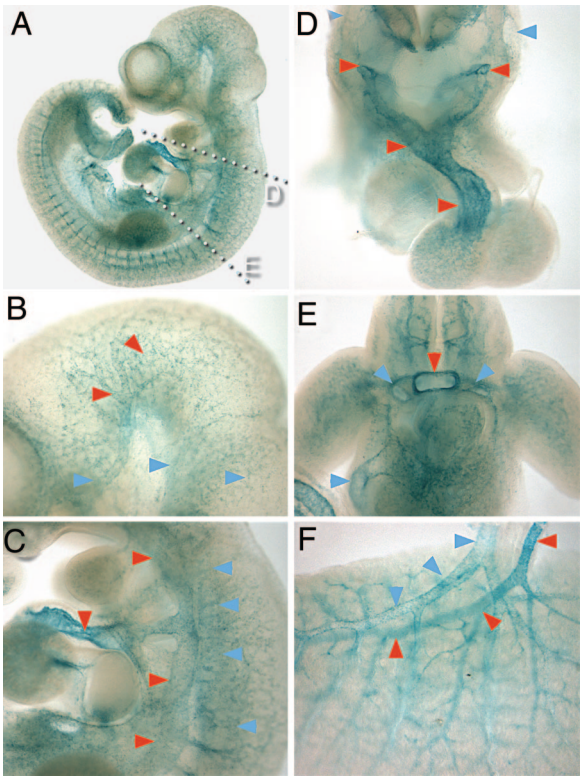

Fig. 4. VE-PTP LacZ reporter gene expression in embryos. (*A–E*) Whole-mount β-gal staining in E10.5 VE-PTP$^{Lz/+}$ embryos. (*A*) The lines depict the level of the cross sections in *D* and *E*. (*B*) Head vasculature showing reporter expression in arteries (red arrows), veins (blue arrows) and capillaries. (*C*) High expression in arterial endothelium (red arrows), especially the aortic sac, outflow tract, and the atrioventricular canal, and lower expression in the cardinal vein (blue arrows). (*D*) Cross section just above the heart, showing expression in the dorsal aortas, third brachial arch artery, aortic sac, outflow tract (red arrows), and anterior cardinal veins (blue arrows). (*E*) Cross section just above the forelimbs, showing expression in the fusing dorsal aortas (red arrow) and cardinal veins (blue arrows). (*F*) Whole-mount β-gal staining in E15.5 VE-PTP$^{Lz/+}$ lung, clearly showing expression in veins (blue arrows) and the stronger expression in arteries (red arrows).

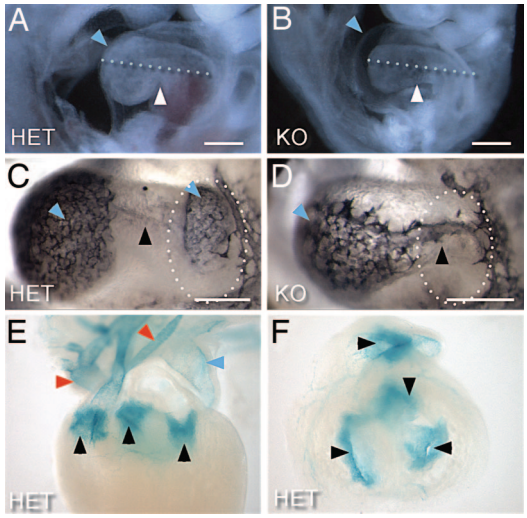

Fig. 5. Cardiac defects and reporter gene expression in VE-PTP$^{Lz/Lz}$ embryos. (*A* and *B*) Freshly dissected E9.5 embryos. VE-PTP$^{Lz/Lz}$ embryos have pericardial edema (blue arrow) (*B*). Although knockout embryos are smaller and developmentally delayed compared with their VE-PTP$^{Lz/+}$ littermates (*A*), their hearts tend to have similar lengths (dotted line is the same length in *A* and *B*). (*C* and *D*) Whole-mount PECAM-1 staining of E9.5 hearts. The pattern in the VE-PTP$^{Lz/+}$ heart (*C*) shows distinct ventricle and atrium staining (blue arrows), as well as staining in the connecting atrioventricular canal (black arrow). In the VE-PTP$^{Lz/Lz}$ heart (*D*), there is only staining in the ventricle (blue arrow) and atrioventricular canal (black arrow), but not in the atrium (dotted circle). (*E* and *F*) Whole-mount β-gal staining in E15.5 VE-PTP$^{Lz/+}$ heart, showing expression in arteries (red arrows), veins (blue arrows), and high expression in all heart valves (black arrows). Heart valves also shown in thick cross section (*F*).

analysis of VE-PTP promoter activity in embryos was conducted up to E15.5. At E9.5, the time when the VE-PTP$^{Lz/Lz}$ cardiovascular defects become apparent, the highest sites of expression are in the aortic sac, outflow tract, umbilical artery, and dorsal aorta (data not shown), with limited or weak expression in smaller-caliber vessels. At E10.5, the strongest expression of the β-gal reporter is still in the endothelium of the heart, including the atrioventricular canal, aortic sac, and outflow tract (Fig. 4 *C* and *D*), dorsal aortas (Fig. 4 *A* and *C–E*), and umbilical arteries (Fig. 4*A*), but it is also strongly expressed in the endothelium of vessels of all sizes, including arteries, capillaries, and somewhat more lightly in veins (Fig. 4 *A–C*). Expression is also observed in the vitelline vessels of the yolk sac (data not shown). At E15.5, β-gal is highly expressed in the heart valves (Fig. 5 *E* and *F*) and continues to be expressed in the endothelium of the major arteries and veins and in the arterioles and venules of organs, with expression being higher in arteries (Fig. 4*F*). This expression in organs correlates with previous results from *in situ* hybridizations done on organs from E15.5 embryos (4). In the adult, expression is very high in the vasculature of lung, spleen, and kidney, as well as in the heart valves, and is also present in the endothelium of arterioles and venules (data not shown).

VE-PTP Heart Defects. In addition to pericardial edema, VE-PTP$^{Lz/Lz}$ embryos have hearts that are relatively enlarged compared with control littermates. At E9.5, although VE-PTP$^{Lz/Lz}$ embryos are significantly smaller than their control littermates, their hearts are of similar size (compare Fig. 5 *B* with *A*). PECAM-1 immunostaining in VE-PTP$^{Lz/+}$ hearts shows the developing ventricles, atria, and connecting atrioventricular canal (Fig. 5*C*). In contrast, VE-PTP$^{Lz/Lz}$ littermates have limited PECAM-1 staining in the relative position of the developing atria (Fig. 5*D*, dotted circle), which may be due in part to the VE-PTP$^{Lz/Lz}$ embryos being developmentally delayed. As previously shown, the outflow tract and the atrioventricular canal is the site of highest expression of the β-gal reporter (Fig. 4*C*). Interestingly, this expression corresponds to the precursors of the developing cardiac valves, and VE-PTP reporter gene expression continues to remain high in all of the developing heart valves (Fig. 5 *E* and *F*) at E15.5. In addition, in adult heart, VE-PTP expression remains high in endothelium covering all of the cardiac valves (data not shown).

VE-PTP Is Expressed in Tumor Vasculature. Subcutaneous implantation of Lewis lung carcinoma cells in adult VE-PTP$^{Lz/+}$ mice causes tumor growth and induces angiogenesis. β-Gal staining shows that VE-PTP is expressed in the newly formed tumor blood vessels (Fig. 6 *A–C*). The tumor invades the overlying skin and coopts the resident vasculature, which leads to the dramatic induction of VE-PTP expression in the coopted vessels (Fig. 6 *B*, *D*, and *E*).

Discussion

Deletion of the VE-PTP gene causes severe cardiovascular defects and embryonic lethality by E10. Because the vascular disruption begins at E9.0, after the primary vasculature is established during vasculogenesis, it appears VE-PTP is not necessary for this process. However, it is required for angiogenesis in embryos, and its absence results in lethality due to defective remodeling. This finding is consistent with previous biochemical studies in which VE-PTP was shown to interact with

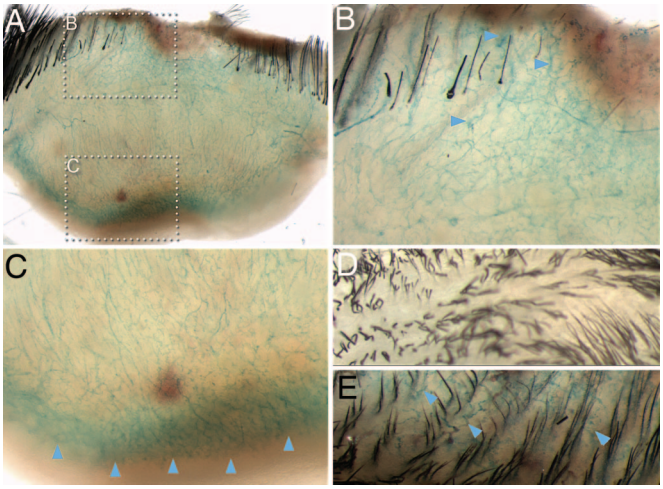

Fig. 6. VE-PTP reporter expression in Lewis lung carcinoma tumors implanted in VE-PTP$^{Lz/+}$ mice. Whole-mount β-gal staining of tumors is shown. (*A*) Thick cross section of the tumor. Boxes depict the areas taken at higher magnification in *B* and *C*. (*B*) Closeup of tumor blood vessels (blue arrows), where it invades the skin. (*C*) Closeup of the tumor edge showing an area with a high concentration of blood vessels (blue arrows). (*D* and *E*) View of the skin surface directly over the tumor (*E*) and from the contralateral side of the mouse (*D*), which shows lacZ-positive vessel growth into the skin (blue arrows).

and dephosphorylate Tie2 (which, like VE-PTP, is critical for angiogenesis but not vasculogenesis) but not VEGF-R2 (4), which has been clearly shown to be critical for vasculogenesis, and in fact, the formation of ECs themselves (10) (see below for further discussion).

During development, the vascular plexus, formed during vasculogenesis, undergoes remodeling and expansion by pruning, coalescence, sprouting angiogenesis (11), and intussusception (12). In VE-PTP mutant embryos, the vascular plexus is established, but it does not remodel correctly. Defects include failure to form branched vascular networks (e.g., in the venous plexus of the head), possibly because of improper pruning and intussusception. Also, the cardinal veins, which form by coalescence of smaller vessels, are indiscernible in VE-PTP mutant embryos, except for partial assembly at its most anterior segment. Instead, the portion of the vascular plexus destined to be cardinal veins remains as a collection of vessels that fail to reshape into a cohesive vessel. The dorsal aortas, which formed normally during vasculogenesis, become stenotic in VE-PTP$^{Lz/Lz}$ embryos. Because the mutant embryos do not have a normal vascular framework, normal blood flow, which is a key component in arterio-venous differentiation (13), is prevented. The VE-PTP$^{Lz/Lz}$ embryos are also developmentally delayed and have pericardial edema, which are indicators of cardiovascular insufficiency. These two characteristics are commonly seen with other gene deletions that cause midgestation lethality because of cardiovascular defects [e.g., VEGF-R3 (14), Dll4 (15–17), and CD148/DEP-1 (3)]. The hearts of VE-PTP$^{Lz/Lz}$ embryos also do not develop properly, which may be due in part to inappropriate vascularization and underdevelopment.

The vascular defects in VE-PTP mutants are most striking in the yolk sac, which completely lacks a remodeled vascular network. Instead, the yolk sac vascular plexus essentially becomes one large vessel fully lined with PECAM-1-positive cells. There is a range in the amount of endodermal and mesodermal detachment in different VE-PTP$^{Lz/Lz}$ yolk sacs. In those that are less detached, the yolk sac is formed of large interconnected channels, and in those more detached, only sparse PECAM-1-positive strands connect the endoderm and mesoderm layers. This variation shows the progression of this vascular defect as a case of unchecked coalescence, where the plexus vessels merge to the point of completely separating the two yolk sac layers, suggesting that VE-PTP plays a role in controlling that remodeling process. Other genes, when deleted, also cause a similar phenotype in yolk sacs (summarized in ref. 18), which has been termed vascular "hyperfusion" (19). Similar hyperfusion defects were described in quail embryos when excessive VEGF was administered, suggesting that this phenomenon can be VEGF driven (19). However, VE-PTP does not appear to play a direct role in the modulation of VEGF-R2, as suggested by prior biochemical data (4) and given the fact that vasculogenesis proceeds normally in VE-PTP mutant embryos. In addition, expression of VE-PTP was low during vasculogenesis and became most highly expressed during angiogenic stages (data not shown and Fig. 4). However, it remains possible that VE-PTP indirectly regulates production of VEGF itself, a possibility not explored in the current study. Thus, the mechanistic role that VE-PTP plays in the hyperfusion process remains unclear.

In embryos, VE-PTP is expressed in both arterial and venous endothelium with the highest apparent levels in arterial vessels and components of the heart. VE-PTP continues to be expressed in adult vascular endothelium, indicating a potential function in vessel maintenance. To explore whether VE-PTP is involved in adult angiogenesis, as occurs during tumor growth, Lewis lung carcinoma cells were xenografted into the flanks of VE-PTP$^{Lz/+}$ mice, and VE-PTP expression was examined in the collected tumors. VE-PTP promoter activity, as evaluated by LacZ expression, was clearly present in the new tumor vessels and was elevated in the vasculature of the skin overlying the tumors, as compared with the control skin on the contralateral flank. These results suggest VE-PTP may be important in tumor angiogenesis, in addition to embryonic angiogenesis, and may in fact represent a novel therapeutic target. Conditional deletion or specific inhibition of VE-PTP during tumor angiogenesis will be necessary to test this hypothesis.

The cardiovascular defects described here for VE-PTP are reminiscent of those reported for the CD148/DEP-1/PTPη mutant mouse, the only other known receptor-type phosphatase expressed (although not exclusively) in ECs (3). In addition, a recently published report (7) describes a distinct VE-PTP mutation, in which an insertion is made between exons 17 and 19, and which results in mice in which the majority of the extracellular region of VE-PTP remains intact and is in fact found to be secreted. It was speculated that this secreted form of VE-PTP ectodomain may represent a neomorphic allele with the potential to retain some function or possibly function in an antagonistic form (7, 8). However, despite the differences in knockout strategy, the described exon 17–19 insertion/deletion and our exon 2–3 deletion mutants appear to have essentially the same spectrum of vascular phenotypes, suggesting that both represent loss of function rather than neomorphic phenotypes.

Tie2 (4) and VE-cadherin (6) have been shown to associate with VE-PTP and as such should be considered, along with any other substrates, as having a role in the mechanism that causes the observed vascular defects. The VE-PTP mutants share many common characteristics with the Tie2 and Ang1 loss-of-function phenotype (20–22). However, deletion of a phosphatase that negatively regulates this signaling pathway would be presumed to have a gain-of-function phenotype rather than to mimic the loss of function of Tie2 or Ang1. Thus, it could be that perturbation of Tie2 signaling in either direction would lead to similar lethal consequences. In allantois explant studies done with ECs from various E8.5 homozygous mutants, it was found that Tie2$^{-/-}$ had normal networks of endothelial cords compared with VE-PTP$^{-/-}$ (7). Further biochemical analysis of the signaling of Tie2 and other VE-PTP targets in VE-PTP-null ECs, as well as the generation of a temporally controlled VE-PTP deletion later in development or in the adult vasculature, will be necessary to further elucidate many of these issues.

Materials and Methods

Targeting the VE-PTP Gene in Mice. Using VelociGene technology (9), an 11.8-kb segment of the VE-PTP gene extending from 27 nucleotides (in exon 2) through exon 3 was replaced with a β-gal reporter gene and a loxP-flanked neomycin selection cassette (pTM-Zen6-loxP). Briefly, a BAC containing the 11.8-kb VE-PTP region to be deleted and 195 kb of flanking sequences (clone 386g24 from a 129/SvJ BAC library from Incyte Genomics, Wilmington, DE) was used to generate a BAC-based targeting vector for replacement of the VE-PTP gene in F1H4 (C57BL/6:129 hybrid) mouse ES cells. Two independent correctly targeted ES cell clones were selected by using the loss of native allele (LONA) assay [as described (9)] and used to generate chimeric male mice. Germ-line transmitting chimeras were bred to C57BL/6 females to generate offspring heterozygous for the modified VE-PTP allele. Timed matings of VE-PTP$^{Lz/+}$ mice and VelociMouse technology (23) were used to generate embryos. The embryos were staged and checked for beating hearts when collected, and the yolk sacs and embryos were photographed during dissection. Yolk sacs and placentas were also collected for analysis. Embryos were genotyped by using the LONA assay. Animals were cared for under the terms and conditions of our Institutional Animal Care and Use Committee.

Quantitative RT-PCR Analysis of VE-PTP and lacZ mRNA Levels. Quantitative RT-PCR (*Taq*Man) was performed as described (24) on an Applied Biosystems (Foster City, CA) 7900HT real-time PCR system. The results are expressed as the ratio of the amount of the RNA of interest to the amount of control RNA (GAPDH) (25) by using specific primers and probes as follows: primers VE-PTP (Ex2–3)-278F, TCAGGATTGTTTCTCTGGATGGA and VE-PTP (Ex2–3)-385R GGGTGGTTGATGCTGTTTTCTC, and probe VE-PTP (Ex2–3)-326T CAGATCCGTTGCCTCC; primers LacZ-33F GGAGTGCGATCTTCCTGAGG and LacZ-102R CGCATCGTAACCGTGCATC and probe LacZ-54T CGATACTGTCGTCGTCCCCTCAAACTG. The analysis was done on RNA extracted from E9.5 embryos (three WT, three VE-PTP$^{Lz/+}$, and four VE-PTP$^{Lz/Lz}$).

Immunostaining and Reporter Detection. Whole-mount embryos, yolk sacs, and placentas, as well as sections of embryos and adult tissues, were immunostained with PECAM-1 antibody to detect vascular endothelium as described (26). Whole-mount embryos, yolk sacs, placentas, and adult tissues, as well as sections of embryos and adult tissues, were stained for lacZ as described (27). Paraffin sections of PECAM-1-stained yolk sacs were counterstained with hematoxylin.

Tumor Implantations. Lewis lung carcinoma cells (American Type Culture Collection, Manassas, VA) were implanted s.c. into the flank of VE-PTP$^{Lz/+}$ mice, and the tumors were collected after 13 days. To visualize reporter expression, whole-mount β-gal staining was done on the tumors and on skin adjacent to the tumor, as well as from the contra-lateral side as described (27).

We thank other Regeneron team members, including Stanley Wiegand, John Rudge, David Frendewey, Thomas M. DeChiara, Aris N. Economides, Yingzi Xue, Wojtek Auerbach, William Poueymirou, Joyce McClain, Sandra Coetzee, and Nicholas Papadopoulos, for assistance in generating the VelociGene ES cells and mice, technical assistance, and many helpful discussions. We also acknowledge the Regeneron executive management and in particular Leonard Schleifer for his ongoing support of this work.

1. Risau W, Flamme I (1995) *Annu Rev Cell Dev Biol* 11:73–91.
2. Coultas L, Chawengsaksophak K, Rossant J (2005) *Nature* 438:937–945.
3. Takahashi T, Takahashi K, St John PL, Fleming PA, Tomemori T, Watanabe T, Abrahamson DR, Drake CJ, Shirasawa T, Daniel TO (2003) *Mol Cell Biol* 23:1817–1831.
4. Fachinger G, Deutsch U, Risau W (1999) *Oncogene* 18:5948–5953.
5. Krueger NX, Streuli M, Saito H (1990) *EMBO J* 9:3241–3252.
6. Nawroth R, Poell G, Ranft A, Kloep S, Samulowitz U, Fachinger G, Golding M, Shima DT, Deutsch U, Vestweber D (2002) *EMBO J* 21:4885–4895.
7. Baumer S, Keller L, Holtmann A, Funke R, August B, Gamp A, Wolburg H, Wolburg-Buchholz K, Deutsch U, Vestweber D (2006) *Blood* 107:4754–4762.
8. Drake CJ, Argraves WS (2006) *Blood* 107:4582.
9. Valenzuela DM, Murphy AJ, Frendewey D, Gale NW, Economides AN, Auerbach W, Poueymirou WT, Adams NC, Rojas J, Yasenchak J, *et al.* (2003) *Nat Biotechnol* 21:652–659.
10. Shalaby F, Rossant J, Yamaguchi TP, Gertsenstein M, Wu XF, Breitman ML, Schuh AC (1995) *Nature* 376:62–66.
11. Risau W (1997) *Nature* 386:671–674.
12. Patan S, Munn LL, Jain RK (1996) *Microvasc Res* 51:260–272.
13. le Noble F, Moyon D, Pardanaud L, Yuan L, Djonov V, Matthijsen R, Breant C, Fleury V, Eichmann A (2004) *Development (Cambridge, UK)* 131:361–375.
14. Dumont DJ, Jussila L, Taipale J, Lymboussaki A, Mustonen T, Pajusola K, Breitman M, Alitalo K (1998) *Science* 282:946–949.
15. Duarte A, Hirashima M, Benedito R, Trindade A, Diniz P, Bekman E, Costa L, Henrique D, Rossant J (2004) *Genes Dev* 18:2474–2478.
16. Gale NW, Dominguez MG, Noguera I, Pan L, Hughes V, Valenzuela DM, Murphy AJ, Adams NC, Lin HC, Holash J, *et al.* (2004) *Proc Natl Acad Sci USA* 101:15949–15954.
17. Krebs LT, Shutter JR, Tanigaki K, Honjo T, Stark KL, Gridley T (2004) *Genes Dev* 18:2469–2473.
18. Argraves WS, Drake CJ (2005) *Anat Rec A Discov Mol Cell Evol Biol* 286:875–884.
19. Drake CJ, Little CD (1995) *Proc Natl Acad Sci USA* 92:7657–7661.
20. Dumont DJ, Gradwohl G, Fong GH, Puri MC, Gertsenstein M, Auerbach A, Breitman ML (1994) *Genes Dev* 8:1897–1909.
21. Sato TN, Tozawa Y, Deutsch U, Wolburg-Buchholz K, Fujiwara Y, Gendron-Maguire M, Gridley T, Wolburg H, Risau W, Qin Y (1995) *Nature* 376:70–74.
22. Suri C, Jones PF, Patan S, Bartunkova S, Maisonpierre PC, Davis S, Sato TN, Yancopoulos GD (1996) *Cell* 87:1171–1180.
23. Poueymirou WT, Auerbach W, Frendewey D, Hickey JF, Escaravage JM, Esau L, Dore AT, Stevens S, Adams NC, Dominguez MG, *et al.* (2006) *Nat Biotechnol* 25:91–99.
24. Livak KJ, Schmittgen TD (2001) *Methods* 25:402–408.
25. Daly C, Wong V, Burova E, Wei Y, Zabski S, Griffiths J, Lai KM, Lin HC, Ioffe E, Yancopoulos GD, *et al.* (2004) *Genes Dev* 18:1060–1071.
26. Gale NW, Thurston G, Hackett SF, Renard R, Wang Q, McClain J, Martin C, Witte C, Witte MH, Jackson D, *et al.* (2002) *Dev Cell* 3:411–423.
27. Adams NC, Gale NW (2006) in *Principles and Practice: Mammalian and Avian Transgenesis–New Approaches*, eds Pease S, Lois C (Springer, Berlin), pp 131–172.